Corrosion in CO$_2$ systems with impurities creating strong acids

Bjørn H. Morland,[†,*,**] *Morten Tjelta,*[**] *Arne Dugstad,*[**] *and Gaute Svenningsen*[**]

*Department of Chemistry, University of Oslo, Sem Sælands vei 26, NO-0371 Oslo, Norway.

**Corrosion Technology department, Instituttveien 18, NO-2007 Kjeller, Norway.

†Corresponding author: Email: bjorn.morland@ife.no.

ABSTRACT

There are several proposed specifications for CO$_2$ transport regarding how much impurities that can be allowed in the CO$_2$ stream. Many of these specifications are based on health, safety and environment (HSE) considerations in case of accidental spill, and only limited focus has been on the pipeline integrity. Previous work has demonstrated that many of the impurities that are expected to be present in CO$_2$ captured from flue gasses may react and form corrosive species.

The present paper studied impurity reactions and corrosion under simulated transport conditions (25 °C and 10 MPa of CO$_2$). An experiment was carried out in a transparent autoclave which allowed for in-situ visual observation. Chemical reactions between the impurities were observed even at very low concentrations (<100 ppmv). These reactions contributed to the production of nitric and sulfuric acid together with formation of elemental sulphur. Corrosion was observed on coupons of carbon steel, but not on stainless steels. The corrosion rate of carbon steel was low, but the amount of acids and solids (corrosion products) produced cannot be accepted from a pipeline integrity perspective. Further experimental studies are needed to determine specific limits for impurity concentrations in captured CO$_2$ for transport.

INTRODUCTION

The carbon dioxide (CO$_2$) concentration in the atmosphere has increased over the last century, mainly due to human activities such as combustion of fossil fuels. Since CO$_2$ contributes to global warming, there is an international agreement to reduce emission of CO$_2$ to the atmosphere.[1] One method to reduce emission is CCS (Carbon Capture and Storage).

In many cases there will be a significant distance between the CO$_2$ capture site and the storage site and the CO$_2$ will be transported in pipelines, by ships or a combination of both. Pipeline transport is regarded as the most cost-effective alternative for large volumes, but for temporary and small storage sites ships might be the preferred method of transportation for offshore storage.[2] USA has routinely transported CO$_2$ from naturally occurring sources in on-shore pipelines for more than 40 years. No serious corrosion problems have been reported, but for captured anthropogenic CO$_2$ the conditions might be different due to the presence of small amounts of other compounds, such as SOx, NOx, O$_2$, H$_2$S, CO. These compounds are referred to as impurities in the present work since CO$_2$ is the main product of the capturing process and anything else would only be present because further cleaning/purification of CO$_2$ is not economically feasible. Although valuable data can be acquired from the existing CO$_2$ transport network, it cannot say much about the effect of the additional impurities and if they may affect the integrity of a pipeline or a ship. There are numerous ways these impurities can react, and many reaction products can potentially form.[3] If all these reactions occurred only in the capture plant it would probably not be a large problem in practice since the reaction products could be removed before the CO$_2$ leaves the plant. However, it is expected that a future CCS network will be more complex, with several capturing plants connected through a joint CO$_2$ transport system. This is proposed in a feasibility study from the Norwegian Ministry of Petroleum and Energy, where the goal is to handle 1.3 million tons/year of CO$_2$ from three different sources and store it in the Smedaheia formation.[2] In cases like this it will be important to avoid cross-impurity reactions that form corrosive species, for example if CO$_2$ streams with different impurities are mixed.

Several papers address the impacts and acceptable concentrations of impurities in the CO$_2$ stream, and several CO$_2$ specifications have been suggested.[4] These specifications are often based on literature studies (see Table 1) and the suggested maximum limits for SOx, NOx, and H$_2$S are commonly based on HSE considerations in case of accidental release of the CO$_2$, while pipeline integrity threats like corrosion or formation of solids were not considered. Thus, there is a lack of experimental data to verify that these limits are safe from a pipeline or ship transport point of view.

Only a limited number of projects have performed experiments with multiple impurities with continuous replenishment,[5-7] and the reported corrosion rates from those experiments were lower than 0.1 mm/y. Several experiments were carried out in closed systems (autoclaves) with batch injection[6-16] of the impurities, usually without replenishment.[6-15, 17-20] The corrosion rates reported are in the range from 0.005 to 7 mm/y, the water saturated experiments tend to report higher corrosion than the under-saturated or fully dissolved water experiments. Since the impurities (except for water) typically were present at a very low concentration (~50 – 200 ppmv) they may have been consumed rapidly if corrosion occurred. This is an issue which can possibly explain why some authors report higher corrosion rates in short duration tests as compared to long term experiments. If the impurities

are consumed by corrosion or chemical reactions during the initial period of exposure, essentially all corrosion will take place in the initial phase after which corrosion might slow down or stop. This will give errors when the mass loss is divided by the full exposure time.

The corrosion mechanism depends on which impurity is present in the experiments but most of the suggested mechanisms[16, 19, 21-23] in the literature follows an absorption of impurity in an existing water film on the surface to create acids like sulfuric/sulfurous, and/or nitric/nitrous acid. The corrosion products often found are $FeSO_3$, $FeCO_3$, Fe_2O_3, and $FeOOH$[12, 16, 19]. Some has also reported $FeSO_4$ [5, 21, 24] and $Fe(NO_3)_3$[19], the latter compound is not common since it is regarded as unstable and instead will usually react to Fe_2O_3[19]. In water-saturated experiments it is likely that a large or thick water film will form, and all the suggested mechanism could be valid. For dissolved water or undersaturated conditions with water concentration as low as 100 ppmv this would not be straight forward, since the water film would consist of only a few monolayers of water[25].

An experimental setup which allows the impurities to be continuously replenished and analyzed during the experiments was used in the present work. This removes uncertainties related to consumption and depletion of impurities due to reactions or corrosion.

The present paper discusses the result of an experiment that was performed in a transparent autoclave with 10 MPa CO_2 containing multiple impurities. The objective was to compare the results with previously published data,[5] to identify if any reactions take place in what is regarded as a safe CO_2 specification and to determine if these reactions may cause corrosion.

EXPERIMENTAL PROCEDURE

The experiment was carried out in an in-house built autoclave with transparent end-plates. The body material was SS316L, with lime soda glass and poly carbonate as the see-through material (Figure 1). The total volume of the autoclave was 330 ml and the maximum design pressure was 29 MPa.

The autoclave had separate injection lines for the different impurities (Figure 2), a measure which prevented the impurities from reacting before entering the autoclave. All lines where of 1/16" tubing to minimize the volume and hence the lag time in the injection and sampling system.

The water was pre-dissolved in the CO_2 (at 10 MPa) before entering the autoclave, meaning that no liquid water was injected in the autoclave at any time. An in-house built moisture generator was used for this purpose. It was an autoclave filled with water. CO_2 was injected at the bottom and moist CO_2 taken out from the top. The water saturated CO_2 was then mixed with dry CO_2 at a given ratio to create the target level of dissolved water. The retention time through the water moisturizer was about 20 hours.

All other impurities were pre-mixed with CO_2 in separate high-pressure precision piston pumps operating at 10 MPa. The impurity stock solutions had concentrations from around 1000 to 3000 ppmv. The injection rates of the piston pumps were adjusted according to the total CO_2 injection rate to get the target impurity concentration in the autoclave. Some minor impurity fluctuations were observed due to day-night temperature variations.

The exhaust CO_2 from the autoclave was depressurized to 0.2 MPa over a heated gas regulator and the flow rate was controlled by a mass flow controller at the low-pressure side. The impurity content of the exhaust CO_2 was analyzed using OFCEAS (Optical Feedback Cavity Enhanced Absorption Spectroscopy) for H_2O, H_2S and O_2. A NDIR/UV photometer was used to measure NO, NO_2 and SO_2, and a zirconium oxide sensor was used as a second O_2 analyzer. Exhaust CO_2 (with impurities) was finally ventilated to a safe area with scrubbers. Gas qualities used in the experiment are listed in Table 2.

Three metal specimens (corrosion coupons) where prepared by grinding up to P1000 paper, rinsing in isopropanol and then cleaning in ultrasonic bath with acetone for 10 minutes, followed by 10 minutes in isopropanol before drying. Three different metals were exposed (Table 3); N10276 (nickel-alloy), S355MC (carbon steel), and S32205 (duplex stainless steel). The coupons were mounted in a holder made from polyether ether ketone (PEEK), as shown in Figure 2, the coupons size was 9.5x9.5 mm. The back side of the carbon steel coupon was covered with mill scale consisting of 5 wt.% wüstite and 95 wt.% magnetite.

When the coupon holder was in place, the autoclave was closed and flushed for several hours with dry low-pressure CO_2 to remove water and oxygen. Then the autoclave was filled with dry CO_2 to a pressure of 10 MPa. Injection of dry CO_2 continued until the measured water concentration was below 5 ppmv. The CO_2 (with impurities) flow rate was 80 g/h. This flow rate did not contribute to significant shear-stresses in the autoclave, and the condition for the metal coupons should be regarded as close to stagnant.

The various impurities were injected sequentially; first H_2O, then SO_2 and O_2, followed by H_2S and finally NO_2. NO_2 was injected in two periods. It started after 98 hours, stopped after 168 hours, started again after 246 hours and then finally stopped after 276 hours. When the concentration of an injected impurity was stable (as measured by the in-situ analyzers), injection of the next impurity was started, and so on, see Table 4 (the brackets indicates the injection order). Possible reactions and corrosion reactions were observed in-situ using a camera, and by analyzing the impurity concentrations in the exhaust CO_2.
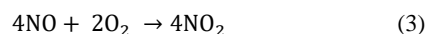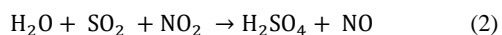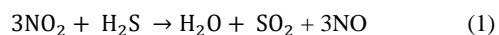
The concentration of impurities in the present work equals about one third of the amount in the previously published experiment[5] but NO_2 was injected in two periods. The presently applied impurity content is well within specifications given in the literature.[4]

The experiment was terminated by purging dry CO_2 through the system for about 20 hours to prevent drop-out of liquids during depressurization. Finally, the system was depressurized, and the autoclave was opened. The coupons were quickly rinsed with distilled water to remove acids and then with isopropanol. Finally, they were dried under nitrogen atmosphere.

The solid products on the metal surface and liquid products in the autoclave were analyzed using energy-dispersive x-ray spectroscopy (EDS), X-Ray Diffraction (XRD), and Ion Chromatography (IC). After investigation on SEM/XRD the carbon coupon was stripped of corrosion film using inhibited hydrochloric acid (Clarke's solution), the other two coupons were only rinsed with isopropanol due to their appearance (they appeared as if unexposed). The coupons were then scanned with a 3D profilometer using white light axial chromatism. The scan grid size was 10 μm x 10 μm. An optical pen with 300 μm vertical range and a vertical resolution of about 12 nm was used.

RESULTS AND DISCUSSION

The experiment was started with injection of CO_2, H_2O, O_2, SO_2 and H_2S. Any significant change in impurity concentrations of the outlet gas, compared to what was fed into the autoclave, would imply that a reaction had taken place. No, or at least very little, chemical reactions were observed for this mixture (from 0 to 98 hours), although slight variations were observed due to diurnal changes of temperature, as shown in Figure 3. The NO_2 injection was started at 98 hours, which resulted in a temporarily increase of H_2O and SO_2 content. The O_2 and H_2S content decreased after NO_2 injection was started, and they remained low as long as NO_2 was injected. This was also observed in previous work.[5] When the H_2S content reached zero, SO_2 started to decrease and NO_2 was detected in the outlet gas. This indicates that at least two reactions were occurring, the first reaction (Eq. 1) consumed H_2S and O_2 while H_2O and SO_2 were produced (Figure 3 between 100 to 110 hours). The second reaction (Eq. 2) consumed H_2O and SO_2 (Figure 3, from 110 to 168 hours) while liquids and solids were produced as observed in Figure 4c. NO was first observed 1.5 hours after the nitrogen dioxide injection started, but it took about 8.5 hours until significant NO_2 concentration was measured. This implies that NO_2 is active in both the first and the second reaction. NO and NO_2 were inversely correlated to each other during the rest of the first NO_2 injection period (Figure 3). Nitrogen monoxide was not injected and must therefore be a reaction product. This inverse correlation might be induced by the presence of oxygen (Eq. 3), were NO and oxygen react and form NO_2. Based on the observations and the fact that NO_2 needs to be present, the following reactions are suggested:

$$3NO_2 + H_2S \rightarrow H_2O + SO_2 + 3NO \qquad (1)$$
$$H_2O + SO_2 + NO_2 \rightarrow H_2SO_4 + NO \qquad (2)$$
$$4NO + 2O_2 \rightarrow 4NO_2 \qquad (3)$$

The dense phase CO_2 inside the autoclave changed from clear to yellow during the first NO_2 injection period (Figure 4) and an additional liquid phase appeared on the walls and the bottom of the autoclave.

After a period without NO_2 injection (Figure 5, from 168 to 248 hours) the initial impurities went back to their original levels. It was observed from the pictures that the liquid at the bottom of the autoclave dried up during this period, and it was completely removed after 50 hours without NO_2 injection. Immediately after the liquid had dried up (at about 217 hours) the concentration of H_2O, O_2, and H_2S increased while SO_2 and NO decreased. NO disappeared completely while SO_2 went back to the initial concentration. The yellow colour gradually disappeared but the visibility in the autoclave got more and more opaque. It is not known if the "cloudiness" was in the bulk of the dense phase CO_2 or on the glass walls only, but in the end when the autoclave was opened the glass walls on the inside had acid "dew" on them.

The second NO_2 injection was started at 248 hours and stopped at 276 hours (Figure 5). A sudden change of cloudiness in the autoclave was observed, the visibility turned more yellow and opaque, due to dew on the glass wall. The impurity measurements showed essentially the same trends as for the first NO_2 injection, but the impurity concentrations were lower and the NO/NO_2 correlation was less clear. NO_2 appeared 26 hours after the injection started (274 hours). This could mean that some products remaining from the first period influenced the reactions in the second period of NO_2 injection. NO was measured immediately after the second NO_2 injection started and remained stable for the rest of the experiment, also after NO_2 injection was stopped. It seems like the amount of "dew" increased when only dry CO_2 was injected towards the end of the experiment (from 276 to 293 hours, see Figure 6) and when the autoclave was depressurized. During depressurization, solubilities are expected to decrease. In the

present case, it is likely that the solubility limit for acids was exceeded since the view inside the autoclave became more opaque (Figure 6B). The glass walls were covered with dew when the autoclave was opened, and it could easily be wiped off. It was not possible to take a liquid sample directly off the glass wall, but a liquid sample from the bottom of the autoclave was analysed using ion chromatography. The analysis showed that the liquid was mostly H_2SO_4 but some HNO_3 was also present (ratio of approximately 10:1). There were also signs of dispersed solids at the autoclave wall.

The results from the IC analysis indicate that there might be a difference in solubility between the acids, suggesting that most of the produced HNO_3 followed the CO_2 stream out of the autoclave while most of the produced H_2SO_4 remained inside the autoclave. Work is in progress to quantify the solubility of HNO_3 and H_2SO_4 in dense phase CO_2, and preliminary results show higher solubility of HNO_3 than of H_2SO_4, in full agreement with the observation in the present work.

The corrosion coupons were "wetted" during the experiment, but the surface did not visually change much, except for the edges of the carbon steel coupon. Sulphur was found on the samples by SEM/EDS investigation (Figure 7), and most of it was found on the carbon steel coupon. Especially around the edges (Figure 8), where the corrosion product layer was thick enough to obtain results with minimum substrate effects. The sulphur containing surface product could be elemental sulphur, iron sulphate or iron sulphide, but it was probably $FeSO_4$, as inferred from the stoichiometric ratios (Table 5). This edge effect could be triggered by either condensation of acid or transfer of liquid (acid) from the coupon holder to the corners of the coupon. The weight loss (Table 6) of the carbon steel coupon amounted to an average corrosion rate of 0.07 mm/y for the whole exposure time. However, Figure 4 (compared with Figure 2) shows that little corrosion occurred before NO_2 was injected. Thus, the corrosion rate could be as high as 0.10 mm/y if only the period after NO_2 injection started counts, still the corrosion rate was be surprisingly low, especially since the coupon was covered with acids. The acid was formed from reaction and would be very concentrated, concentrated acid is not as corrosive as diluted[26, 27] and the maximum corrosion rate is somewhere in the middle of very diluted and concentrated H_2SO_4. However, the hygroscopic effect of the acids would attract water to the wetted surface from the CO_2 and dilute the acids which would lead to more corrosion. The amount of liquid acid is decisive, small amounts could be saturated with corrosion products faster and passivate the steel by creating a layer on the surface. There are some uncertainties regarding the corrosion rate given for the carbon steel coupon. The mill scale side is not included in the calculation of the corrosion rate since visual inspection revealed little attack on this side. During removal of corrosion products with Clarke's solution, some of the mill scale could have fallen off and contributed to a weight loss higher than the actual corrosion attack. The sum of these uncertainties might lead to a lower corrosion rate than the one reported. The original plan for the experiment was to observe reactions and products of reaction, the steel coupons were added merely as a screening test and this is the reason for the unfavourable carbon steel scale still being present. Negligible corrosion was found on the coupons of nickel-alloy and duplex stainless steel, supported by the weight loss data (Table 6) and visual inspection. However, we note that some sulphur-rich particles were found on the surfaces.

XRD-analysis of the products on the carbon steel coupon was nonconclusive, either because of a low quantity of products or the product might be of amorphous nature. Dugstad et al.[5] did also report $FeSO_4$ and sulphur at three times higher concentrations, still they could not perform XRD due to little corrosion products on the coupons. Even when the coupons were wetted with produced acid and a lump of sulphur was found inside the autoclave. This shows the huge difference

between low level of dissolved water and water-saturated experiments. There is no thick water film present to absorb the impurities, the sample gets wetted by acid produced in reactions between the impurities in the dense phase CO_2 or at the surfaces inside the autoclave. Figure 6 shows a cloud of acid inside the autoclave. The acid is newly formed and concentrated, and hence, it is likely that $FeSO_4$ can be found at the surface of the carbon steel sample since the surface reaction would be between H_2SO_4/HNO_3 and the carbon steel. Limitation of the EDS analysis could have prohibited the finding of nitrogen to indicate $Fe(NO_3)_x$, or the $Fe(NO_3)_x$ was so unstable that Fe_2O_3 formed instead as reported by Sun et al.[19] Presence of mainly $FeSO_4$ can be inferred from EDS analysis (Table 5), and the IC results supports that mostly H_2SO_4 was present in the liquid phase. It is however, not clear if the presence of H_2SO_4 will hamper the attack from HNO_3. As protection in form of corrosion film, the denser packed $FeSO_4$ would give more passivation of corrosion than the loosely formed Fe_2O_3 (or $Fe(NO_3)_x$) product[9, 19, 24], this might be the reason for the low corrosion rate in the present paper. The production of HNO_3 is not fully understood, but one possible route might be through the H_2SO_4 liquid phase formed inside the autoclave. Water could have absorbed in the acid and accumulated, the NO_2 would then have an aqueous phase to absorb into which leads to the typical reaction for forming nitric acid (Eq. 4):

$$3NO_2(g) + H_2O(l) \rightarrow 2HNO_3(l) + NO(g) \qquad (4)$$

The first 100 hours, with CO_2, H_2O, SO_2, O_2, and H_2S should, from a CO_2 specification point of view, be regarded as safe at the given concentrations. Even though no quantifiable data can be presented in this paper from this period, the qualitative evidence in form of over five hundred pictures showing no change at any of the coupon's surfaces. No droplet shaped attacks should appear with these concentrations as long as the water injection is pre-dissolved in the CO_2 before entering the autoclave and not injected as liquid water.

3D scanning of the exposed and stripped corrosion coupons revealed not pitting or localised attacks (Figure 9), except some topography that was introduced by sample preparation before the experiment was started. This was also supported by a visual examination.

Although the overall results are relatively clear with H_2O, H_2S, O_2, NO_2 and SO_2 reacting to give nitric acid, sulfuric acid and elemental sulphur, the detailed reactions are not yet fully understood. Work is in progress to investigate these reactions. Nevertheless, it is known that these strong acids are corrosive to carbon steel and they may therefore pose an integrity threat for a CO_2 transport pipeline.

CONCLUSIONS

The experiment clearly demonstrated that dense phase CO_2 (10 MPa, 25°C) with impurities H_2O, SO_2, H_2S, O_2, and NO_2 well within a recent CO_2 specification[4] (Table 1) reacted in and formed HNO_3, H_2SO_4, and small amounts of elemental sulphur.

❖ No reactions were observed in the absence of NO_2.

❖ Negligible corrosion was found on the coupons of nickel-alloy and duplex stainless steel, although some sulphur-rich particles were found on their surfaces.

❖ Corrosion products, possible $FeSO_4$, was observed on the carbon steel coupon and the corrosion rate was 0.07 mm/y.

❖ No localised attacks were observed.

❖ From an integrity point of view the impurity combination tested in this experiment must be avoided in a CO_2 transport system since the produced sulfuric and nitric acid could damage the pipeline. Formation of solid products, like $FeSO_4$ and elemental sulphur could lead to clogging problems.

References

1. IPCC, "Climate Change 2013: The Physical Science Basis.," (Cambridge University Press, Cambridge, United Kingdom and New York, NY, USA, 2013).
2. Gassco, Gassnova, *Ministry of Petroleum and Energy, Norway*, (2016):
3. M. Halseid, A. Dugstad, B. Morland, *Energy Procedia* 63, (2014): p. 2557-2569.
4. S. Herron, P. Myles, "Quality guidelines for energy system studies - CO_2 impurity design Parameters," DOE/N/NETL-341/011212, (2013).
5. A. Dugstad, M. Halseid, B. Morland, *Energy Procedia* 63, (2014): p. 2547-2556.
6. O. Yevtushenko, R. Bäßler, I. Carrillo-Salgado, "Corrosion stability of piping steels in a circulating supercritical impure CO_2 environment," CORROSION/2013, paper no. 2372 (Houston, TX: NACE International, 2013).
7. H. Rütters, "COORAL – CO_2 purity for capture and storage," 7th CO2GeoNet Open Forum, 2012).
8. A. Dugstad, M. Halseid, B. Morland, S. Clausen, "Dense phase CO_2 transport – When is corrosion a threat," Northern Area Western Conference/2011, (Houston, TX: NACE International, 2011).
9. A. Dugstad, M. Halseid, B. Morland, A.O. Sivertsen, "Corrosion in dense phase CO_2 with small amounts of SO_2, NO_2 and water," (Eurocorr 2012, 2012).
10. J. Brown, B. Graver, E. Gulbrandsen, A. Dugstad, B. Morland, *Energy Procedia* 63, (2014): p. 2432-2441.
11. F. Farelas, Y.S. Choi, S. Nesic, "Effects of CO_2 phase change, SO_2 content and flow on the corrosion of CO_2 transmission pipeline steel," CORROSION/2012, paper no. 1322 (Houston, TX: NACE International, 2012).
12. Y.-S. Choi, S. Nesic, "Effect of water content on the corrosion behavior of carbon steel in supercritical CO_2 phase with impurities," CORROSION/2011, (Houston, TX: NACE International, 2011).
13. Y. Xiang, Z. Wang, C. Xu, C. Zhou, Z. Li, W. Ni, *The Journal of Supercritical Fluids* 58, 2 (2011): p. 286-294.
14. A. Dugstad, M. Halseid, B. Morland, "Corrosion in dense phase CO_2 pipelines – State of the art," Eurocorr 2011, paper no. 4954 2011).
15. A. Dugstad, S. Clausen, B. Morland, "Transport of dense phase CO_2 In C-steel pipelines - When is corrosion an issue?," CORROSION/2011, (Houston, TX: NACE International, 2011).
16. Y. Hua, R. Barker, A. Neville, *Corrosion* 71, 5 (2015): p. 667-683.

17. C. Sun, J. Sun, S. Liu, Y. Wang, *Corrosion Science* 137, (2018): p. 151-162.
18. C. Sun, J. Sun, Y. Wang, X. Lin, X. Li, X. Cheng, H. Liu, *Corrosion Science* 107, (2016): p. 193-203.
19. C. Sun, Y. Wang, J. Sun, X. Lin, X. Li, H. Liu, X. Cheng, *The Journal of Supercritical Fluids* 116, (2016): p. 70-82.
20. J. Sun, C. Sun, G. Zhang, X. Li, W. Zhao, T. Jiang, H. Liu, X. Cheng, Y. Wang, *Corrosion Science* 107, Supplement C (2016): p. 31-40.
21. Y.-S. Choi, S. Nesic, D. Young, *Environmental Science & Technology* 44, 23 (2010): p. 9233-9238.
22. Y. Xiang, M. Xu, Y.-S.J.C.E. Choi, Science, Technology, 52, 7 (2017): p. 485-509.
23. A. Kranzmann, T. Neddemeyer, A.S. Ruhl, D. Huenert, D. Bettge, G. Oder, R.S. Neumann, *International Journal of Greenhouse Gas Control* 5, Supplement 1, (2011): p. S168-S178.
24. A. Dugstad, M. Halseid, B. Morland, *Energy Procedia* 37, (2013): p. 2877-2887.
25. C. Leygraf, *P. Marcus, J. Oudar (Eds.), Corrosion Mechanisms in Theory and Practice*, (New York: 1995).
26. Z. Panossian, N.L.d. Almeida, R.M.F.d. Sousa, G.d.S. Pimenta, L.B.S. Marques, *Corrosion Science* 58, (2012): p. 1-11.
27. G.H. Damon, *Industrial & Engineering Chemistry* 33, 1 (1941): p. 67-69.

FIGURE CAPTIONS

FIGURE 1. Photo showing the camera and the transparent autoclave with dosing and analyzing lines connected.

FIGURE 2. Photo of the inside of the autoclave with separate injection lines for the different impurities and holder with corrosion coupons. Coupon A was N10276 (nickel-alloy), coupon B was S355MC (carbon steel), and coupon C was S32205 (duplex stainless steel).

FIGURE 3. Impurity concentrations in the outlet gas for the initial period and the first injection period of NO_2 (98 to 168 hours).

FIGURE 4. In-situ images inside the autoclave at different exposure times. Picture A was taken before the NO_2 injection was started, picture B was taken 1 hour after injection of NO_2 had started, and picture C was taken 69 hours after the NO_2 injection had started.

FIGURE 5. Impurity concentrations in the outlet gas after stopping the first NO_2 injection. The second period with NO_2 injection started from 247 hours. All impurities were stopped at 276 hours.

FIGURE 6. "Dew" on the glass walls at the end of the experiment (A) and during the depressurization (B).

FIGURE 7. SEM images of the exposed corrosion coupons.

FIGURE 8. SEM image (top) and EDS analysis of the edge of the carbon steel coupon.

FIGURE 9. Surface profile of corrosion coupons after removal of corrosion products.

TABLE CAPTIONS

TABLE 1: Range of impurity concentrations from literature.[4]
TABLE 2: Gas qualities used in experiment.
TABLE 3: Chemical composition of the metal coupons.
TABLE 4: Experimental conditions.
TABLE 5: EDS analysis.
TABLE 6: Weight loss measurements.

TABLE 1: Range of impurity concentrations from literature.[4]

Compound	Concentrations in literature (ppmv)	Recommendation (ppmv)
H_2O	20 – 650	500
O_2	10 – 40000	10
SOx	10 – 50000*	100
H_2S	20 – 13000*	100
NOx	20 – 2500*	100

*These concentrations are often given as 100 ppmv for HSE reasons.

TABLE 2: Gas qualities used in the experiment.

Gas type	Quality
CO_2	5.0
NO_2	2.0
SO_2	3.0
H_2S	2.8
O_2	5.0

TABLE 3: Chemical composition of the corrosion coupons.

Element	C	Ti	Mn	P	S	V	Nb	Si	Al
S355MC*	< 0.12	< 0.15	< 1.5	< 0.025	< 0.02	< 0.2	< 0.09	< 0.5	> 0.015

Element	C	Cr	Mn	P	S	Ni	Mo	Si	N
S32205*	<0.3	22.0-23.0	<2.0	<0.03	<0.02	4.5-6.5	3-3.5	<1.0	0.14-0.2

Element	Fe	Cr	Mn	P	Co	V	Mo	Si	W
N10276**	4.0-7.0	14.5-16.5	<1.0	<0.04	<2.5	<0.35	15.0-17.0	<0.08	3.0-4.5

*The balance is iron.
**The balance is nickel.

TABLE 4: Experimental conditions.

H_2O (ppmv)	O_2 (ppmv)	SO_2 (ppmv)	H_2S (ppmv)	NO_2 (ppmv)	Temperature (°C)	Pressure (MPa)	Flow rate (g/h)
90 (1*)	70 (1*)	30 (1*)	36 (2*)	32 (3*)	25	9.8	80

*The number in the brackets indicate the injection order

TABLE 5: Result of EDS analysis.

Point no.	O (atomic%)	S (atomic%)	Fe (atomic%)
1	78.9	14.1	6.9
2	67.7	17.2	15.1
3	74.9	17.2	7.9
4	69.7	20.7	9.6
5	68.4	17.3	14.4
6	70.0	17.8	12.2
7	70.0	17.7	12.3

TABLE 6: Weight loss measurements.

	N10276	S32205	S355MC
Before exposure (g)	0.6007	2.0198	2.8287
After exposure (g)	0.6007	2.0198	2.8296
After stripping (g)	0.6007*	2.0198*	2.8268
Mass loss (mg/cm^2)	0	0	1.8

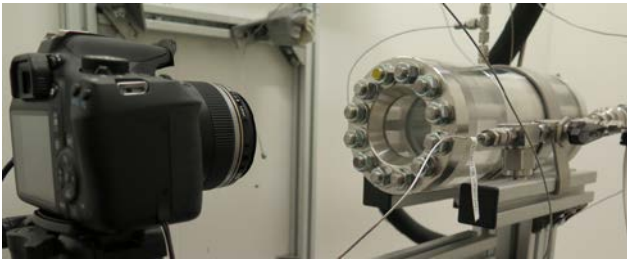*Stripped with ultrasonication isopropanol only, due to appearance.

FIGURE 1. Photo showing the camera and the transparent autoclave with dosing and analyzing lines connected.
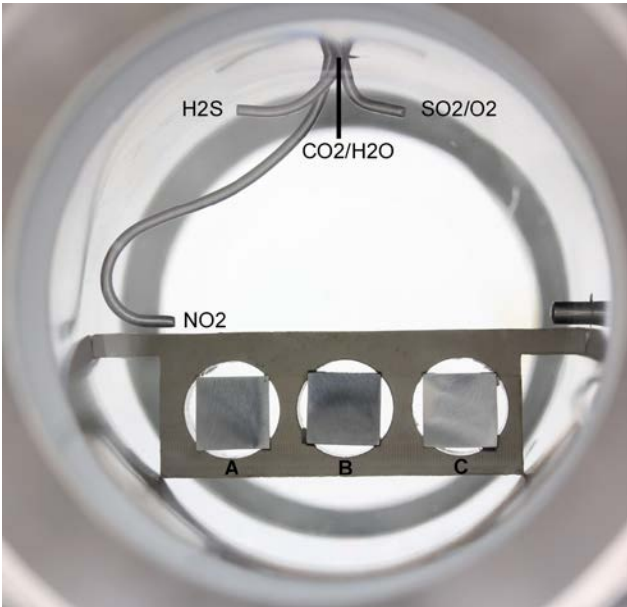

FIGURE 2. Photo of the inside of the autoclave with separate injection lines for the different impurities and holder with corrosion coupons. Coupon A was N10276 (nickel-alloy), coupon B was S355MC (carbon steel), and coupon C was S32205 (duplex stainless steel).
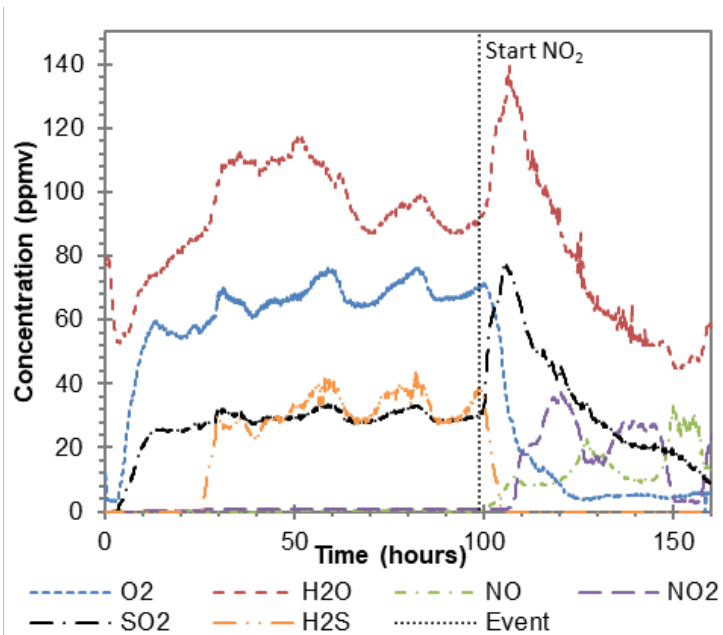

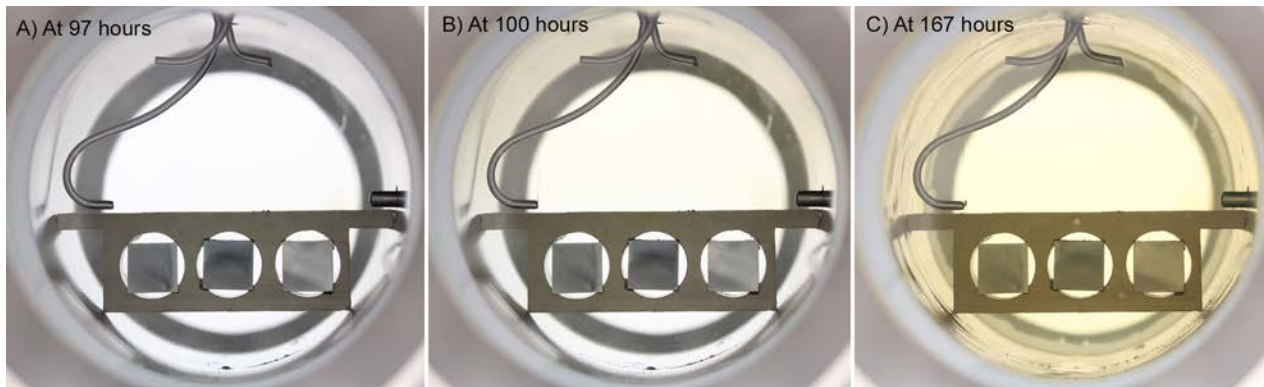FIGURE 3. Impurity concentrations in the outlet gas for the initial period and the first injection period of NO_2 (98 to 168 hours).

FIGURE 4. In-situ images inside the autoclave at different exposure times. Picture A was taken before the NO_2 injection was started, picture B was taken 1 hour after injection of NO_2 had started, and picture C was taken 69 hours after the NO_2 injection had started.

FIGURE 5. Impurity concentrations in the outlet gas after stopping the first NO_2 injection. The second period with NO_2 injection started from 247 hours. All impurities were stopped at 276 hours.
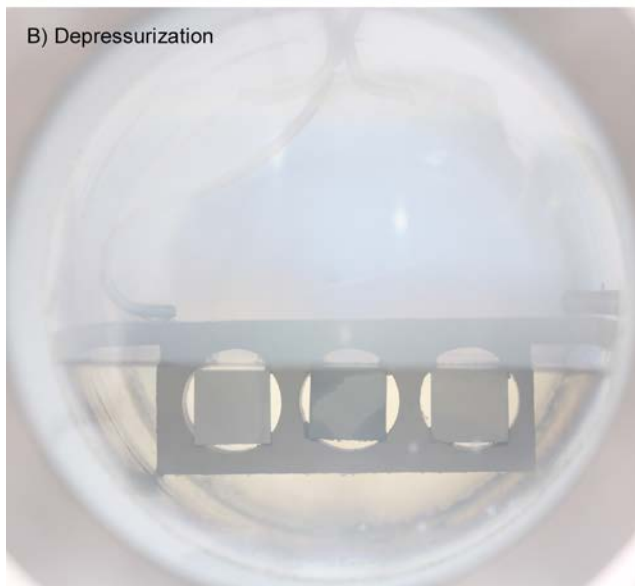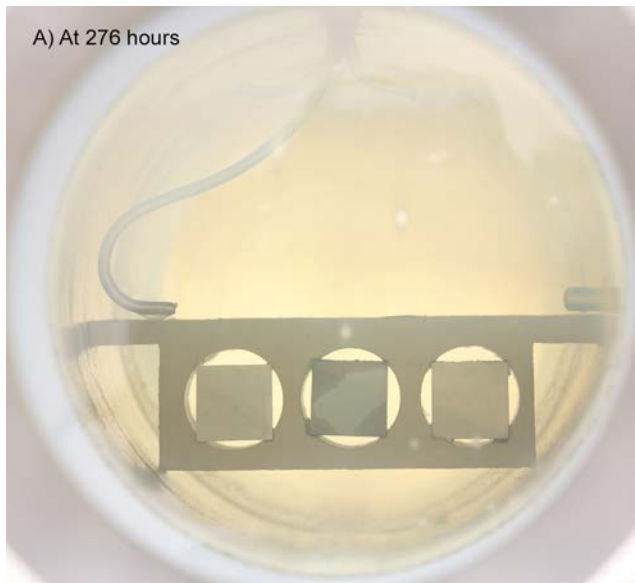
FIGURE 6. "Dew" on the glass walls at the end of the experiment (A) and during the depressurization (B).
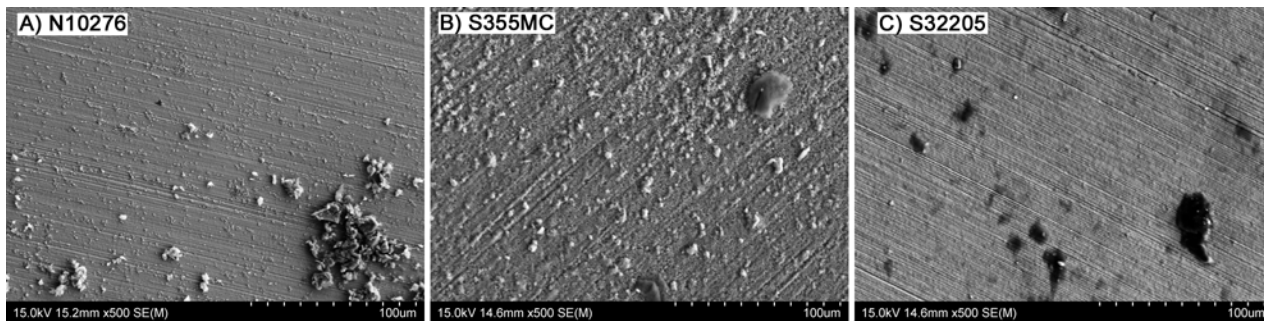

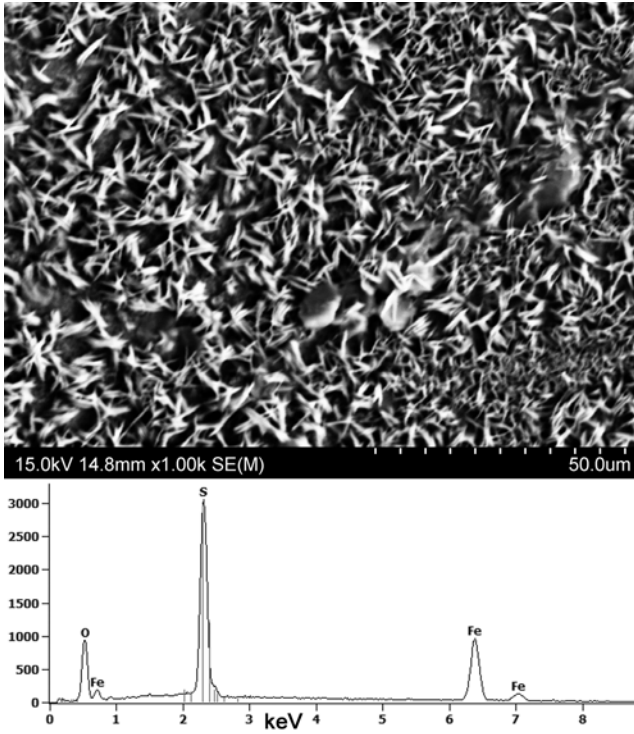FIGURE 7. SEM images of the exposed corrosion coupons.

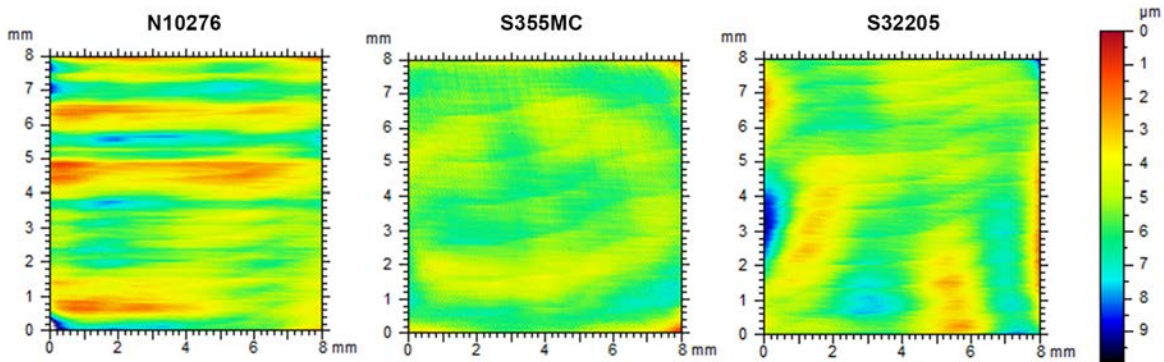FIGURE 8. SEM image (top) and EDS analysis of the edge of the carbon steel coupon.

FIGURE 9. 3D surface profile of corrosion coupons after removal of corrosion products.